DOI: 10.1002/chem.200800683

Novel Hybrid Materials Consisting of Regioregular Poly(3-octylthiophene)s Covalently Attached to Single-Wall Carbon Nanotubes

Andreas A. Stefopoulos,[a, b] Christos L. Chochos,[a, c] Maurizio Prato,[d] George Pistolis,[e] Kostas Papagelis,[f] Foteini Petraki,[b, g] Stella Kennou,[b, g] and Joannis K. Kallitsis*[a, b]

Abstract: Facile routes for the synthesis of hybrid materials consisting of regioregular poly(3-octylthiophene)s covalently attached to single-wall carbon nanotubes are presented for the first time. These materials are easily processable using common organic solvents, and at the same time combine the properties of regioregular poly(3-alkylthiophene)s with those of single-wall carbon nanotubes. Moreover, studies of the properties of these materials have provided strong evidence for an electron transfer from the regioregular poly(3-octylthiophene) to the single-wall carbon nanotube.

Keywords: conjugated polymers · electron transfer · nanotubes · photovoltaics · solar cells

Introduction

The discovery of photoinduced electron transfer between conjugated polymers and fullerene (C_{60})[1] and the optimized photovoltaic devices fabricated from regioregular poly(3-hexylthiophene)s (rrP3HT) and a soluble derivative of fullerene (PCBM),[2] opened new possibilities for the fabrication of flexible photovoltaics (PVs) based on semiconducting polymers. The demand for further optimization of the PV efficiency has stimulated an intensive research effort both for new low-band-gap polymeric materials,[3] capable of serving as electron donors, and for new efficient electron-accepting materials. As regards the latter, carbon nanotubes (CNTs) have gained interest as an alternative to the fullerene derivatives, because their nanometer dimensions enable charge transport along the long axis of their carbon structures and can contribute to a reduced probability of back-transfer to the oxidized electron-donor polymer. The first report of a polymer/SWNTs photovoltaic device was in 2002,[4] which concerned composites of SWNTs with regioregular poly(3-octylthiophene) (rrP3OT). Since then, many efforts aimed at the fabrication of CNT-based photovoltaic devices have been reported.[5] However, limited power conversion efficiencies were found. Thus, several obstacles need to be properly addressed, such as the processability of the nanotubes and the selection of an appropriate set of electron donors to facilitate higher power conversion efficiencies from such photovoltaic devices.

The initial disadvantage of poor solubility of CNTs has been partially overcome by various functionalization techniques[6] based on either the covalent attachment[7] of different organic groups to the π-conjugated backbone of the SWNTs through appropriate reactions or the noncovalent absorption[8] or wrapping of various functional polymers.[9]

[a] A. A. Stefopoulos, Dr. C. L. Chochos, Prof. J. K. Kallitsis
Department of Chemistry, University of Patras
26504 Patras (Greece)
Fax: (+30) 261-099-7122
E-mail: j.kallitsis@chemistry.upatras.gr

[b] A. A. Stefopoulos, F. Petraki, Prof. S. Kennou, Prof. J. K. Kallitsis
Foundation for Research and Technology Hellas
Institute of Chemical Engineering
and High Temperature Processes (FORTH-ICEHT)
P.O. Box 1414, 26504 Patras (Greece)

[c] Dr. C. L. Chochos
Advent Technologies, Patras Science Park
26504 Patras (Greece)

[d] Prof. M. Prato
Dipartimento di Scienze Farmaceutiche
Università di Trieste
Piazzale Europa 1, 34127 Trieste (Italy)

[e] Dr. G. Pistolis
Institute of Physical Chemistry, NRCS Demokritos
15310 Athens (Greece)

[f] Dr. K. Papagelis
Department of Materials Science, University of Patras
26504 Rio, Patras (Greece)

[g] F. Petraki, Prof. S. Kennou
Department of Chemical Engineering, University of Patras
26504 Patras (Greece)

Supporting information for this article is available on the WWW under http://dx.doi.org/10.1002/chem.200800683.

"Grafting to"[10a] or "grafting from"[10b] techniques have also been used for the conventional polymer modification of nanotubes. In order to prevent the disruption of π-conjugation, various modifications[11] that allow weak functionalization of the SWNTs, resulting in the lowest possible distortion of their electronic properties, can be used.

The main objective of this work was to find a synthetic method for functionalizing CNTs with regioregular poly(3-alkylthiophene)s (rrP3ATs). In this regard, we present for the first time the synthesis of easily processable hybrid materials consisting of rrP3OT covalently attached to SWNTs. Using suitably monofunctionalized rrP3OT, we have investigated its direct attachment to the SWNT surface by two different synthetic routes, as shown in Schemes 1 and 2. We chose to use rrP3OT for this work due to the superior optoelectronic properties and chemical stability of the rrP3ATs and the improved processability of the synthesized materials because of the long alkyl chains of P3OT. The materials obtained have been characterized by thermogravimetric analysis (TGA), Raman and Fourier-transform infrared (FTIR) spectroscopies, UV/Vis spectrophotometry, steady-state photoluminescence spectroscopy, and by X-ray and UV photoelectron spectroscopies (XPS and UPS). Strong evidence for an electron transfer from the rrP3OT to the SWNT has been obtained, considering the results obtained from the application of all of the aforementioned techniques. This gives a first indication that these materials fulfill the prerequisites as promising candidates for photovoltaic applications.

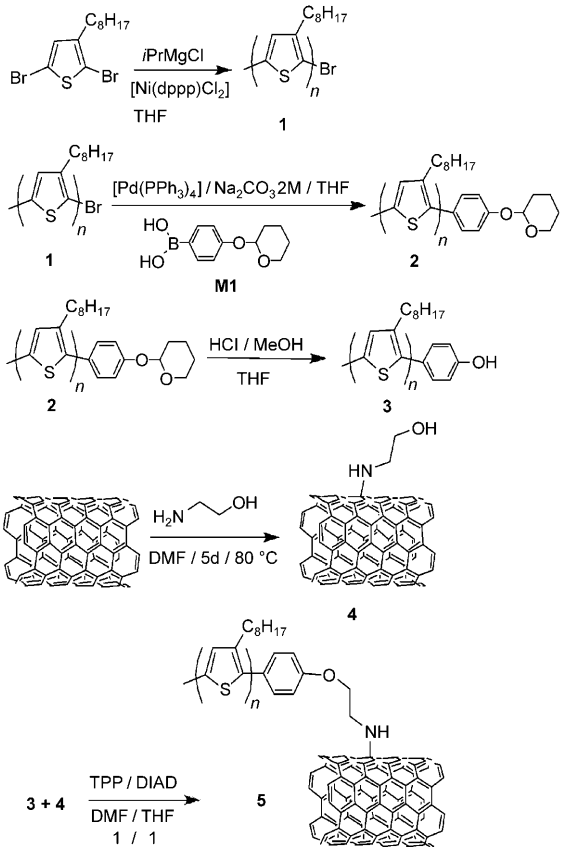

Scheme 1. Synthetic route towards regioregular poly(3-octylthiophene)-modified single-wall carbon nanotube **5**.

Results and Discussion

The first goal of this work was the preparation of rrP3OT functionalized at one end with terminal phenol groups. The approach that we used was a two-step process that differed slightly from the one reported by McCullough et al.[12] for the end-functionalization of rrP3ATs, in order to avoid the synthesis of difunctionalized phenol-terminated rrP3ATs. First, we synthesized and isolated the H/Br-terminated rrP3OT **1**, as described in the Experimental Section. The ^{1}H NMR spectrum of **1** is presented in Figure 1a, which allows accurate determination of its molecular weight based on the relative integrals of the peak at $\delta = 2.8$ ppm, assigned to the α-methylene protons of the octyl groups (a), and the broad peak at $\delta = 2.6$–2.5 ppm, assigned to the methylene protons on the first carbon substituent (b and b′) on the end units. For example, the number of repeat units n for the polymer **1** is equal to 13, corresponding to $M_n = 2600$. This molecular weight is lower than that obtained from GPC measurements ($M_n \approx 4350$), in agreement with previous findings.[12] Subsequently, **1** was subjected to a palladium-mediated Suzuki coupling reaction[13] with **M1** in order to prepare the phenoxy-tetrahydropyranyl-terminated rrP3OT **2** (Scheme 1). The ^{1}H NMR spectrum of **2** is shown in Figure 1b. The characteristic peaks of the tetrahydropyranyl protecting group as well as two small doublet peaks attributable to the phenyl ring at $\delta \approx 7.4$ and 7.1 ppm can clearly be observed. Monofunctionalization of the rrP3OT was also confirmed by the ^{1}H NMR spectrum shown in Figure 1b. Based on the peak at 1.9 ppm assigned to the protons of the tetrahydropyranyl group and the peak at 0.9 ppm assigned to the methyl protons of the octyl group, a degree of polymerization of 15 repeating units was estimated for this polymer, which is close to the $DP_n = 13$ obtained for rrP3OT **1**. Finally, hydrolysis of **2** with 37% hydrochloric acid afforded the desired compound **3** in quantitative yield.

The reaction of pristine SWNTs with 2-aminoethanol in DMF led to the synthesis of **4**, which has free hydroxyl groups at the periphery of the SWNT. The direct reaction of amino derivatives at the surface of carbon nanotubes has been described in the literature,[11b,14] and offers a facile route for preparing functionalized carbon nanotube materials. Based on the TGA results shown in Figure 2, the pristine SWNT and compound **4** display weight losses of about 8 and 17.5%, respectively, at 800 °C. This corresponds to the presence of one functional hydroxy-terminated group per 60 carbon atoms.

Raman spectroscopy is one of the most extensively employed methods for probing the modification of the electronic and vibrational properties of carbon nanotubes caused by various chemical functionalization strategies. Figure 3a shows Raman spectra, normalized to the G-band intensity, of pristine and aminoethanol-modified SWNTs. For

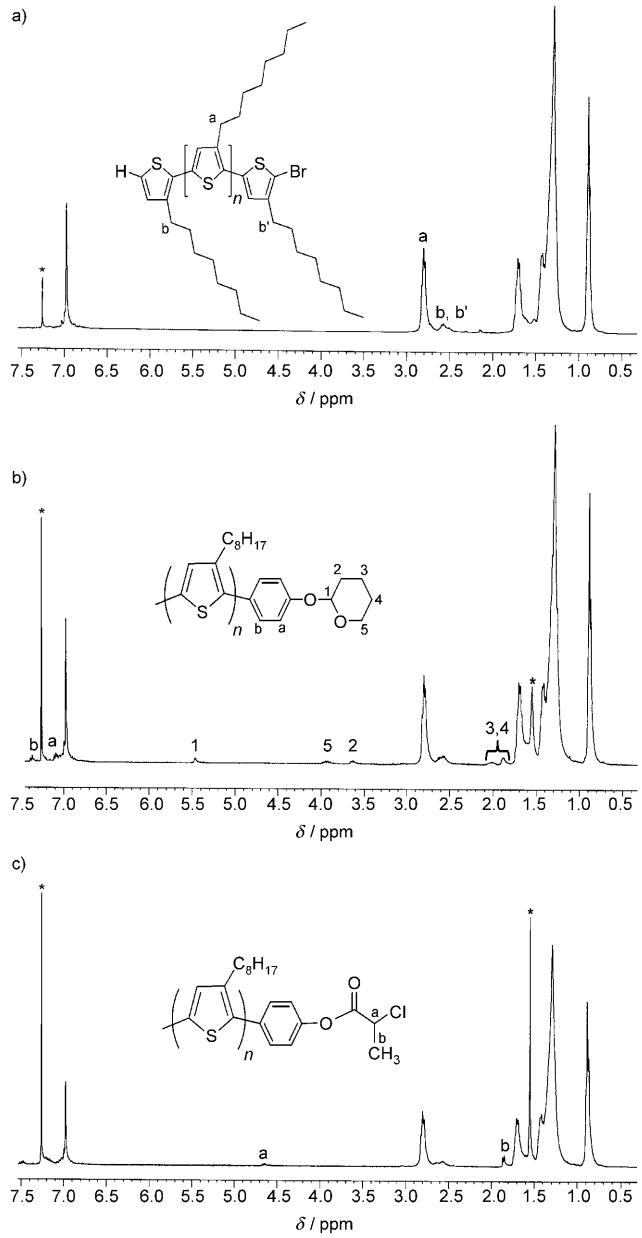

Figure 1. ^{1}H NMR spectra (400 MHz) of a) rrP3OT **1**, b) phenoxy-tetrahydropyranyl-terminated rrP3OT **2**, and c) rrP3OT macroinitiator **6**. The asterisk denotes the solvent.

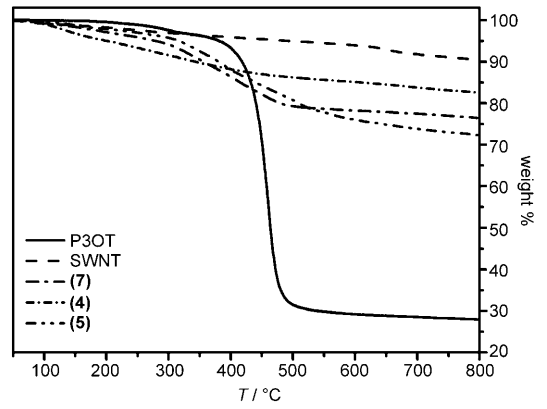

Figure 2. TGA curves of pristine **SWNT**, the rrP3OT **1**, the nanotube derivative **4**, the rrP3OT-co-SWNT **5**, and the rrP3OT-SWNT **7** (10 °C min^{-1} under nitrogen atmosphere).

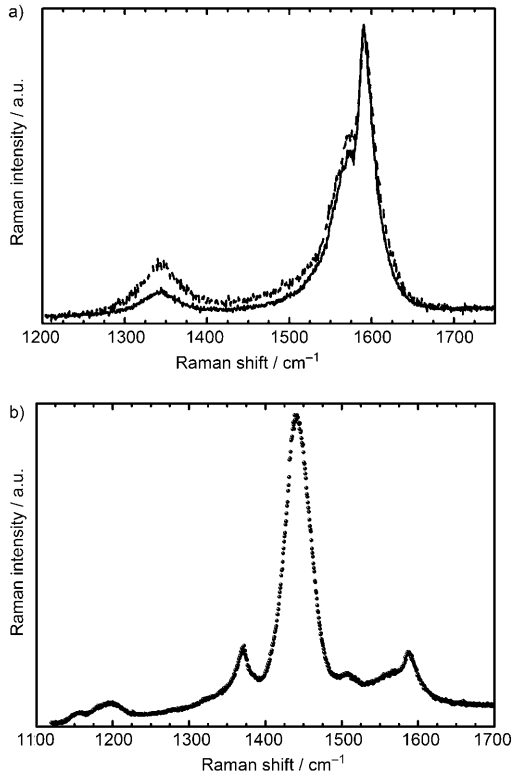

Figure 3. a) Normalized Raman spectra of the washed pristine (——) SWNT material (see text) and the aminoethanol-modified (-----) SWNT, excited at 514.5 nm. b) Raman spectrum of rrP3OT-co-SWNT **5**, excited at 514.5 nm.

a valid comparison, the same protocol leading to the synthesis of **4** was followed for the raw SWNT material in the absence of 2-aminoethanol.

The high-frequency region spectrum of pristine SWNTs contains three main components. The features located at $\approx$1592 cm^{-1} and $\approx$1565 cm^{-1} constitute the so-called G-band resulting from the tangential C–C vibrations both longitudinally (G$^+$-band) and transversally (G$^-$-band) on the axis of the nanotube. The weak feature at around 1343 cm^{-1}, the so-called D-band, involves scattering of an electron through phonon emission by the disordered sp^2 network. The intensity ratio between the D- and G-bands is commonly used to characterize the degree of nanotube functionalization. Any changes on the nanotube walls that affect its structural periodicity, namely vacancies, covalent bond formation, or disorder of any kind in the graphitic lattice may enhance the D-band scattering.[15] The Raman spectrum of aminoethanol-modified SWNT **4** shows similar features to those of the washed pristine material. However, after the reaction of SWNTs with amino derivatives, the D-band intensity is significantly increased compared to the washed pristine

sample. The intensity ratio $I(D)/(I(G^+)+I(G^-))$ exhibits a significant enhancement of $\approx 30\%$, suggesting a conversion of a substantial amount of sp^2- to sp^3-hybridized carbon due to the introduction of covalently bound amino groups within the nanotube framework.

Decoration of the modified SWNT **4** with the phenol-terminated rrP3OT **3** was accomplished by an ether bond formation in the presence of triphenylphosphine (TPP) and diisopropylazodicarboxylate (DIAD) (Mitsunobu-type reaction),[16] providing compound **5**. The amount of the polymer chemically bonded to **4** was evaluated by TGA (Figure 2). The aminoethanol-modified SWNT **4** showed very good thermal stability up to 800 °C under an inert nitrogen atmosphere, while the presence of the grafted polymer in **5** is verified by the occurrence of polymer decomposition in this temperature range. TGA measurements demonstrated that the polythiophene precursor accounted for approximately 11 wt% of **5**. Considering the molecular weight of the polymer of 2600, the functionalization percentage of rrP3OT-co-SWNT **5** was estimated to be approximately 0.12%. A simple calculation yields a maximum functionalization percentage of 1.9% if all the hydroxyl groups of derivative **4** are connected to units of phenol-terminated rrP3OT **3**. This indicates that not all of the hydroxyl groups of the derivative **4** had reacted with the phenol groups of **3**, and we estimate that there was an average of one regioregular polythiophene chain per 17 aminoethanol groups.

In the second synthetic route (Scheme 2), esterification of the free phenol group of **3** with 2-chloropropionyl chloride furnished the desired macroinitiator **6**. The ^{1}H NMR spectrum of **6** is depicted in Figure 1c, which clearly shows the disappearance of the characteristic signals of the tetrahydropyranyl protecting group and the concomitant appearance of new peaks at $\delta \approx 4.6$ and 1.8 ppm, which may be assigned to the proton next to the halogen atom and the methyl protons of the chloropropionyl group, respectively. The degree of polymerization of the rrP3OT **1** was further corroborated by the ^{1}H NMR spectrum in Figure 1c. Based on the methyl protons of the chloropropionyl group and the methyl protons of the octyl group, a degree of polymerization of 15 repeating units was obtained for this polymer, in agreement with the $DP_n = 15$ obtained for the phenoxy-tetrahydropyranyl-terminated rrP3OT **2**.

A method for introducing fullerene into a polymer backbone that has been reported in the literature involves atom-transfer radical polymerization conditions.[17] By employing similar conditions for the reaction between **6** and SWNT, we succeeded in synthesizing the functionalized rrP3OT-SWNT **7**. The amount of polymer grafted onto the surface of the SWNT was estimated by TGA (Figure 2). TGA measurements demonstrated that approximately 15 wt% of **7** was due to the polythiophene chains, corresponding to a functionalization percentage of 0.09%. The degree of functionalization in both cases was about 0.1%, a value that is significantly higher than that quoted in a recent report[18] concerning the preparation of polymer-modified nanohorns under anionic polymerization conditions.

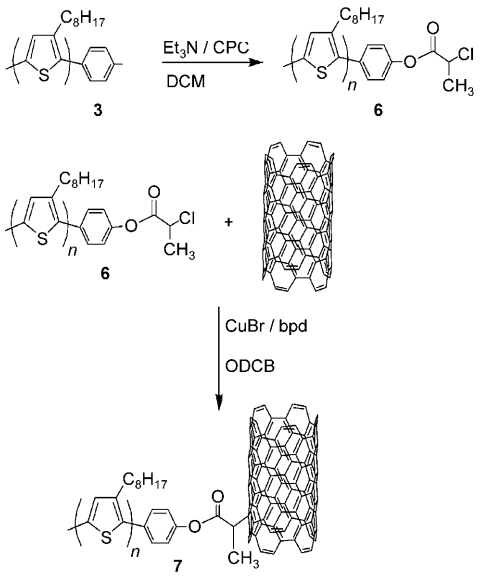

Scheme 2. Synthetic route towards regioregular poly(3-octylthiophene)-modified single-wall carbon nanotube **7**.

Figure 3b presents the Raman spectrum of **5** excited at 514.5 nm, in which contributions from both the nanotubes (see also Figure 3a) and the rrP3OT can clearly be observed. The peaks at $\tilde{\nu}$ 1369, 1442, and 1514 cm^{-1} may be attributed to vibrations within the polymeric chains.[19] The Raman spectrum is dominated by the mode at 1442 cm^{-1}, which can be assigned to a C=C symmetric stretching deformation of the thiophene ring.[19] At a laser power of 0.4 mW, the neat rrP3OT sample shows the appearance of intense luminescence light accompanied by visible damage to the sample surface at the illumination spot. The polymeric Raman peaks could only be detected at a laser power of less than 0.02 mW. In this case, the characteristic Raman features were poorly resolved on top of a huge luminescence background in the observed Raman spectrum. This behavior, in combination with the absence of a luminescence signal from rrP3OT-co-SWNT **5**, indicates significant SWNT–polymer interactions, resulting in efficient polymer photoluminescence quenching. It is important to note that SWNT/rrP3OT blend, with the same percentage of rrP3OT by weight as **5**, exhibits similar behavior to that observed for **5**, suggesting that the polymer did not have to be directly attached on the SWNT surface, but that the polymer chains could interact non-covalently with the sidewalls.

Investigation of the low-frequency radial breathing mode (RBM) region, in which all of the tube atoms vibrate radially in phase, gives valuable information concerning the binding of addends on SWNTs. Figure 4 shows the room temperature Raman spectra of pristine SWNT, rrP3OT-co-SWNT **5**, and rrP3OT/SWNT blend in the RBM region. In the case of pristine SWNT (Figure 4a), many discrete RBM peaks can clearly be observed, reflecting the presence of a wide distribution of SWNT diameters. The dominant RBM peak for the pristine sample is that at ≈ 190 cm^{-1}, attributable to

tubes of 1.29 nm in diameter.[20] Despite the fact that Raman scattering originating from the polymer chains themselves contributes to the spectrum of the functionalized material, the RBM bands of the modified tubes (Figure 4b) display strong intensity attenuation compared to the unmodified ones (Figure 4a). Only the peak located at $\approx 190\ cm^{-1}$ in the spectrum of the pristine material remains clearly resolved, exhibiting a frequency upshift of $\approx 6\ cm^{-1}$ in the modified sample. The results obtained reveal that the proposed functionalization scheme causes substantial alterations to the electronic band structure, significantly reducing the resonance enhancement of the Raman scattering, and/or modifies the overall symmetry and the bonding strength of the tubes. Moreover, it is evident from Figure 4c that the spectrum obtained from the control experiment exhibits a less pronounced loss of scattering intensity compared to that of **5**, although there is significant intensity redistribution of the RBM peaks. Also, the aforementioned peak of the pristine sample at $\approx 190\ cm^{-1}$ is subject to a quite small shift of $\approx 1\ cm^{-1}$. The observed changes in the RBM modes of the rrP3OT/SWNT blend can be rationalized by considering non-covalent interactions between the polymer and the graphite sheet.

FTIR characterization was also used to verify the attachment of the rrP3OT precursor on the SWNT surface in both **5** and **7**. The spectrum of rrP3OT **1** show peaks at 2926 and 2853 cm^{-1}, attributable to the methyl and methylene protons of the octyl side chain group (Figure 5), while the IR spectra of materials **5** and **7** feature similar peaks at 2926 and 2853 cm^{-1}, respectively (Figure 5).

The UV/Vis and emission spectra of **1**, both in solution and the solid state, are shown in Figure S1 (see the Supporting Information). The UV/Vis spectra of **1** display an absorption maximum at 440 nm in solution and at 512, 554, and 606 nm in the solid state (Figure S1a), characteristic of rrP3ATs.[21] In addition, the photoluminescence spectra of **1** exhibit two electronic transitions, at 572 and 620 nm in solution and at 650 and 715 nm in the solid state, respectively (Figure S1b).

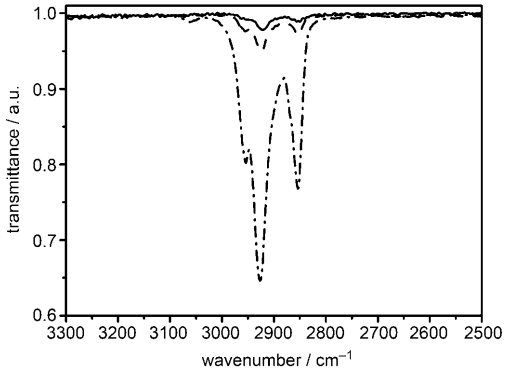

Figure 5. FTIR spectra of rrP3OT **1** (–•–•), rrP3OT-co-SWNT **5** (-----), and rrP3OT-SWNT **7** (——) in the 3300–2500 cm^{-1} region.

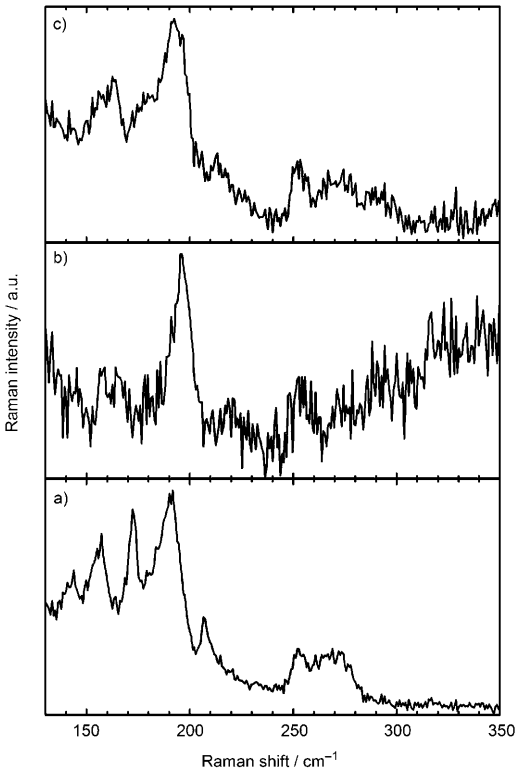

Figure 4. Raman spectra of a) pristine SWNTs, b) rrP3OT-co-SWNT **5**, and c) rrP3OT/SWNT blend at 514.5 nm excitation.

The UV/Vis spectra of **5** and **7** in the solid state are shown in Figure 6a. Strong evidence for efficient attachment of the polythiophene precursor to the SWNT is provided by the corresponding absorption spectra. Although SWNTs do not show any absorption band between 400 and 700 nm in the solid state, the functionalized materials **5** and **7** display broad absorption bands between 400 and 700 nm attributable to the rrP3OTs. Furthermore, it is shown that the absorption spectra of the rrP3OTs are less resolved when they are attached to the SWNTs, as compared to the spectra of the regioregular polythiophene precursors. In addition, comparing the emission spectra of the modified **5** or **7** in the solid state with those of the rrP3OT thin film, one can see that although the absorption spectra are adjusted to almost the same absorption value, the emission from **5** or **7** is totally quenched (Figure 6b), in agreement with the results obtained from the Raman measurements.

The XP spectra of the C1s core level for the rrP3OT-co-SWNT **5**, the SWNT/rrP3OT blend, the pristine SWNT, and the P3OT film are shown in Figure 7. All XP spectra were fitted with mixed Gaussian–Lorentzian peaks after Shirley background subtraction. The C1s peak of the pristine SWNT (Figure 7d) is found at a binding energy of 284.6 eV, with a full-width at half-maximum (FWHM) of 1.15 eV. The spectrum consists of three components: one sharp peak at 284.6 eV, which is assigned to sp^2 carbon; a broad tail near 285 eV, which indicates the presence of sp^3 carbon; and a small satellite peak that differs in energy from the main

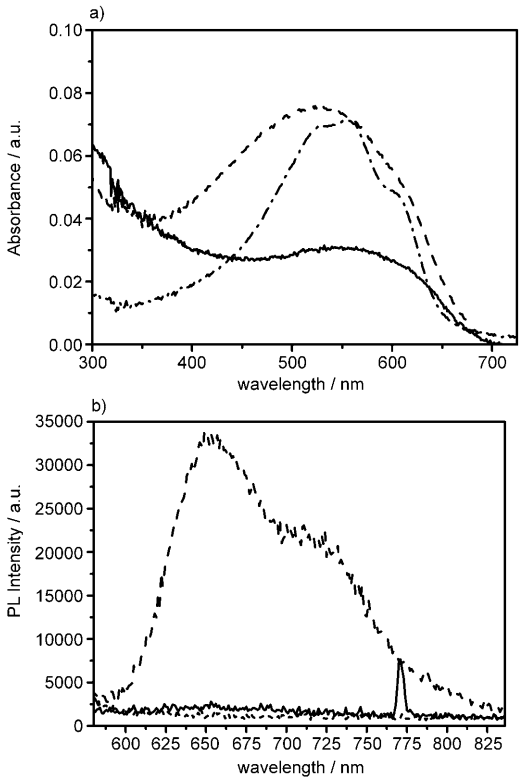

Figure 6. a) UV/Vis and b) photoluminescence spectra of rrP3OT **1** (–•–•), rrP3OT-co-SWNT **5** (-----), and rrP3OT-SWNT **7** (——) in the solid state.

peak by about 5.5 eV, which is a loss feature corresponding to π-plasma excitation, in agreement with literature data.[22,23] In the spectrum of the rrP3OT film, the C1s core level is measured at 285.1 eV, with an FWHM of 1.5 eV (Figure 7c), and the S2p level is at 164.1 eV (not shown), in agreement with previous observations for similar films.[24] If the C1s XP spectrum is fitted with two components (285 and 286.7 eV) with an energy separation of 1.7 eV and an area ratio of 6:1, whereby the low-binding-energy peak relates to a C=C−C environment and the high-binding-energy peak relates to a C=C−S environment,[25] there exists a residual signal which requires the addition of a third component at 285.2 eV. Accordingly, the peak at 285.2 eV is attributed to an extra carbon concentration, which is present on the surface of the film due to its exposure to the atmosphere.

The C1s XPS peak for material **5** is broader (FWHM 1.5 eV) and it appears at a binding energy of 284.90 eV, 0.3 eV higher than that for the pristine SWNT (Figure 7a). Four components are used in the fitting, two (284.60 and 285.60 eV) for the SWNT contribution (the satellite feature is completely quenched) and two (285.10 and 286.80 eV) for the rrP3OT. Figure 7b shows the C1s XP peak for the corresponding blend. This peak is situated at 284.70 eV with an FWHM of 1.30 eV. It is also fitted by two groups of peaks because of the SWNT and rrP3OT contributions (in this case, a small satellite contribution is still present). A comparison of the total areas of the SWNT and rrP3OT components in Figures 7a and b shows that the rrP3OT contribution in **5** exceeds 60%, whereas in the blend the SWNT contribution dominates, amounting to about 65%. This indicates that the rrP3OT in **5** has a tendency to cover the SWNT, which leads to a more intimate contact and possibly facilitates electronic interaction.

Figure 8 shows the C1s XP peaks of the SWNT, the SWNT/rrP3OT blend, and **5** over a wider binding energy range, in which the plasmon peak is clearly shown. The plasmon peak disappears in the case of **5**, which is an indication

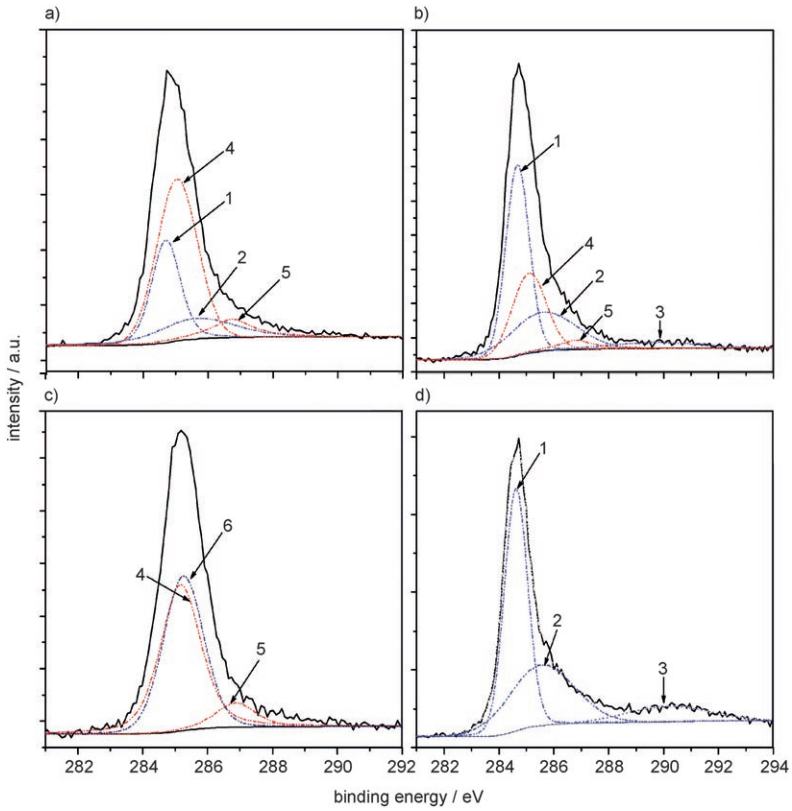

Figure 7. C1s XPS peaks of a) the rrP3OT-co-SWNT **5**, b) SWNT/rrP3OT blend, c) rrP3OT film, and d) pristine SWNT. The fitting of the XP spectra consists of the following components (dashed lines): 1) that at 284.6 eV binding energy is assigned to sp^2 carbon, 2) that at 285.6 eV corresponds to sp^3 carbon, 3) that at 290.1 eV corresponds to π-plasma excitation, 4) that at 285.0 eV is related to C=C−C bonds, 5) that at 286.7 eV is related to C=C−S bonding, and 6) that at 285.2 eV is attributed to atmospheric contamination.

that the features of the carbon nanotube are changed, since the plasmon peak is related to the curved nature of the graphene sheets in the nanotubes.[22] In the case of the blend, this feature is still present, albeit with lower intensity than in the pristine SWNT, which means that the carbon nanotube contribution is still high enough compared to **5**, in agreement with the results obtained from the abovementioned analysis of the C1s peaks.

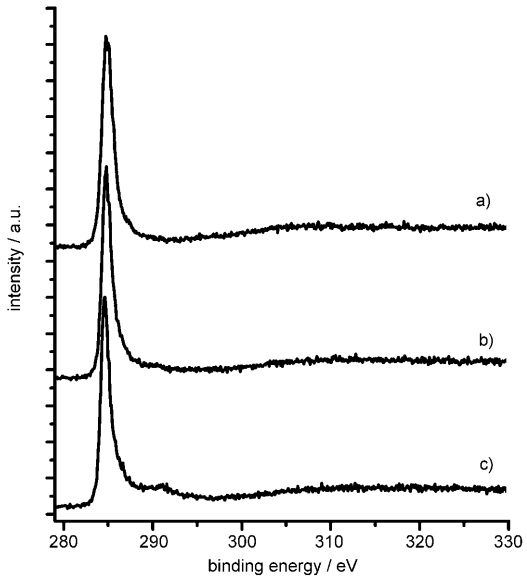

Figure 8. C1s XPS peak in a wider binding energy range, in which the plasmon peak is clearly shown, for a) SWNT, b) rrP3OT/SWNT blend, and c) rrP3OT-co-SWNT **5**.

The valence bands of the SWNT, the rrP3OT-co-SWNT **5**, and the SWNT/rrP3OT blend, as measured by UPS, are shown in Figure 9a, while a more detailed view near the low-binding-energy region, which also includes the rrP3OT valence band, is shown in Figure 9b. The prominent peak of the SWNT valence band, which extends up to the Fermi edge cut-off, is observed at a binding energy of 3 eV from the Fermi level and may be attributed to π-band states, as reported in previous studies.[23]

The low-binding-energy region of the rrP3OT film, up to 4 eV, contains only π contributions from the conjugated backbone, which are related to the electronic structure of the polymer.[24] The HOMO position is measured at 1 eV from the Fermi level ($E_\beta = 0$). The valence band of **5** shows a peak at about 3.5 eV with lower intensity and a HOMO position at about 0.5 eV, which indicates that the modification affects the electronic structure of the carbon nanotubes, shifting the Fermi level upwards. In the case of the SWNT/rrP3OT blend, the peak is quite strong; it is located at about 3.2 eV and there is still density of states near the Fermi edge, which means that the carbon nanotube features are still present. The work function value decreases from 4.7 eV for the pristine SWNT to 4.4 eV for the blend and to 4.2 eV for **5**. This lowering of the work function is an indication of a partial charge transfer from the rrP3OT to the carbon nanotubes.

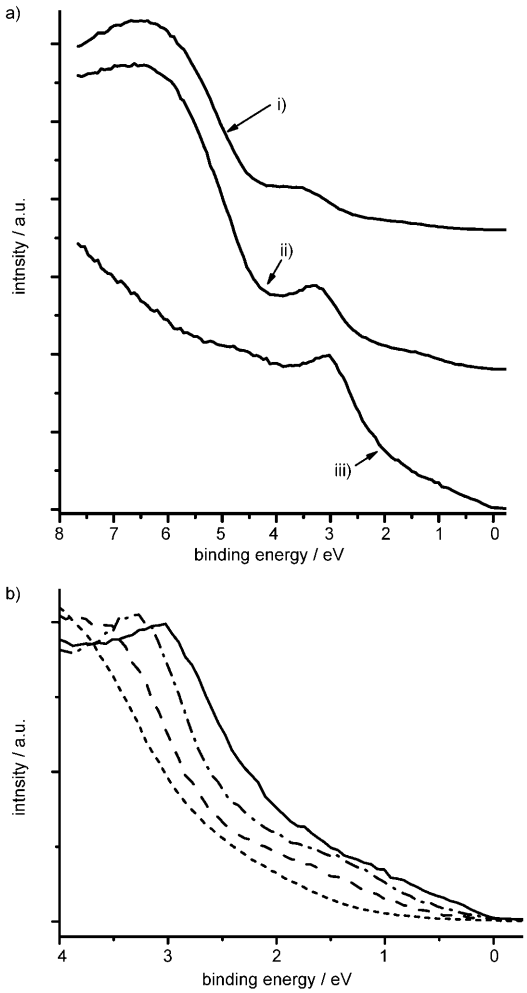

Figure 9. a) UPS spectra of i) rrP3OT-co-SWNT **5**, ii) rrP3OT/SWNT blend and iii) SWNT. b) A detailed view of the valence band near the low-binding-energy region of SWNT (——), rrP3OT-co-SWNT **5** (-----), rrP3OT/SWNT blend (–•–•), and rrP3OT (– – –).

A correlation of the XPS and UPS results shows that the chemical modification of the SWNT by rrP3OT affects the electronic structure of the carbon nanotubes, decreasing the work function value, as rrP3OT covers a large area of the carbon nanotubes. In a blend with the same percentage of rrP3OT by weight, the features of the carbon nanotubes are less affected and the influence of the rrP3OT does not significantly alter their electronic structure.

Conclusion

In summary, novel materials consisting of rrP3OT covalently attached to SWNT have been effectively synthesized. These have been extensively characterized using a variety of spectroscopic techniques, such as TGA, Raman, FTIR, UV/Vis, steady-state photoluminescence, XPS, and UPS. These

hybrid materials are easily processable since they are completely dispersable in common organic solvents, while all of the relevant experimental observations indicate an electron transfer from the excited polythiophene chains to the SWNT backbone, showing that this type of modification does not significantly disturb the electronic properties of the SWNT, while at the same time the processability of the nanotube is greatly improved. Using this methodology, we can efficiently synthesize hybrid materials that combine the outstanding physicochemical properties of SWNTs with those of rrP3ATs, which can be expected to find application in practical optoelectronic devices.

Experimental Section

Instrumentation and measurements: The structures of the synthesized materials were clarified by ^{1}H NMR spectroscopy using a Bruker Avance DPX 400 MHz spectrometer. Gel-permeation chromatography (GPC) was carried out at 25 °C using a Polymer Lab chromatographer with two Ultra Styragel linear columns (10^4, 500 A), a UV detector, polystyrene standards, and $CHCl_3$ as eluent at a flow rate of 1 mL min^{-1}. Centrifugation was performed using a Hettich Zentrifugen Universal 320 centrifuge, and sonication was carried out with a Bransonic (Branson) 2510 model ultrasonic cleaner. TGA experiments were performed on a Q50 series TA instrument. The degree of functionalization of compound **4** was estimated according to the formula: (% carbon/atomic weight of carbon)/(% functional group/molecular weight of the functional group). Raman spectra were recorded using a microscope equipped with a triple monochromator combined with a Peltier cooled charge-coupled device detector system. The spectra were acquired in the back-scattering geometry using the 514.5 nm excitation line provided by an argon laser. The light was focused on the sample using an 80× objective. The data were recorded at a laser power of 0.4 mW, measured directly before the sample, in order to minimize heating effects. To avoid problems related to inhomogeneities in the samples, all spectra were acquired from three to five different spots for each sample. The phonon frequencies were obtained by fitting Lorentzian line shapes to the experimental peaks. Transmission FTIR spectra were recorded using a BRUKER Tensor-27 spectrometer. Photoelectron spectroscopy measurements were carried out in a commercial ultra-high vacuum (UHV) system consisting of fast entry specimen assembly, preparation, and analysis chambers. The analysis chamber was equipped with a hemispherical electron analyzer (SPECS LH-10), a twin-anode X-ray gun, and a discharge lamp for X-ray and UV photoelectron spectroscopy (XPS and UPS) measurements. The base pressure was 5×10^{-10} mbar. XPS measurements were made with the unmonochromated $Mg_{K\alpha}$ line at 1253.6 eV and a constant analyzer pass energy of 36 eV, while HeI (21.22 eV) radiation was used for UPS. The spectrometer was calibrated by reference to the Au4f$_{7/2}$ core level (84.00 ± 0.05 eV) for a clean Au foil. The XPS resolution, measured from the full-width at half-maximum (FWHM) of the Au4f$_{7/2}$ line, was 1.10 eV for a constant pass energy of 36 eV. The analyzer resolution for the UPS measurements was determined from the width of the Au Fermi edge, and was found to be 0.16 eV. A negative bias of 12.30 V was applied to the sample during UPS measurements in order to separate sample and analyzer high-binding-energy cut-offs and to estimate the absolute work function from the UV photoemission spectra. Detailed XPS and UPS measurements were carried out on the system **5** (rrP3OT covalently attached to SWNT; P3OT-co-SWNT). For comparison, pristine single-wall carbon nanotubes (NANOCYL S.A.; SWNT purity > 90 wt %), an SWNT/rrP3OT blend with the same percentage by weight of rrP3OT, as well as an rrP3OT film obtained by spin coating from a 1 mg mL^{-1} solution of the polymer in chloroform were also investigated. UV/Vis spectra were recorded on both Hewlett Packard 8452 A diode-array and Perkin-Elmer Lambda-16 spectrophotometers. Steady-state fluorescence spectra were measured with an Edinburgh Instruments Model FS-900 spectrofluorimeter. The excitation wavelength was 450 nm for solution measurements and 514 nm for those in the solid state. The samples for the UV/Vis and photoluminescence experiments were prepared as follows: **5** or **7** (1 mg) was dissolved in 1,1,2,2-tetrachloroethane (10 mL) and the solution was sonicated for 1 h. Then, uniform thin films of the above materials were prepared by slow evaporation of the solvent from the substrate (quartz plates 2.5 cm × 2.5 cm × 1.5 mm thick) in a desiccator using a mechanical pump. Moreover, thin films of rrP3OT **1** were prepared following the same procedure as described above for **5** or **7**, but starting by injecting 6 μL of a concentrated solution of **1** (1 mg) in 1,1,2,2-tetrachloroethane (1 mL) into pure 1,1,2,2-tetrachloroethane (3 mL).

Monomer and polymer synthesis: All solvents and reagents were purchased from Aldrich and were used without further purification unless otherwise stated. The SWNTs used in this work were obtained from NANOCYL S.A. (SWNT purity > 90 wt %). All reactions were performed under an inert atmosphere (argon). Tetrahydrofuran (THF) was distilled from benzophenone and metallic sodium; dimethylformamide (DMF) was distilled from calcium hydride. 2,5-Dibromo-3-octylthiophene[26a] and 4-(tetrahydro-2*H*-pyranyloxy)phenylboronic acid **M1**[26b] were synthesized according to published procedures. The synthesis of the H/Br-rrP3OT **1** was based on synthetic procedures reported in the literature[26a,27] and involved the Ni-catalyzed chain-growth polymerization of 2-bromo-3-octylthiophene-5-magnesium bromide. The crude polymer was fractionated by Soxhlet extraction with solvents of an increasing ability to solubilize P3OT (methanol, acetone, hexane, and chloroform). The polymer was isolated from the hexane extract. ^{1}H NMR (400 MHz, $CDCl_3$): $\delta = 0.89$ (t, 3H), 1.29 (m, 8H), 1.40 (m, 2H), 1.69 (t, 2H), 2.80 (t, 2H), 6.98 ppm (s, 1H); GPC: M_n: 4350, PDI: 1.7; ^{1}H NMR: $DP_n = 13$, M_n: 2600.

Synthesis of phenoxy-tetrahydropyranyl terminated rrP3OT (2): A reaction flask was charged with rrP3OT **1** (1 g), **M1** (1.211 g, 5.454 mmol), and tetrakis(triphenylphosphine)palladium [$Pd(PPh_3)_4$] (126 mg). The flask was degassed and filled with argon several times. THF (100 mL) and 2 M Na_2CO_3 (6.1 mL) were then added and the mixture was heated at reflux for 48 h under an argon atmosphere. Thereafter, the solvent was partially removed under reduced pressure and the concentrated mixture was poured into methanol to precipitate the crude polymer. The polymer was collected by filtration and washed by a series of Soxhlet extractions with methanol, acetone (in order to remove the excess **M1**), and chloroform. Polymer **2** (0.91 g) was recovered from the chloroform extract. ^{1}H NMR (400 MHz, $CDCl_3$): $\delta = 0.88$ (t, 45H), 1.31 (m, 120H), 1.42 (m, 30H), 1.70 (t, 30H), 1.88 (br, 2H), 2.01 (br, 2H), 2.81 (t, 30H), 3.63 (m, 2H), 3.94 (m, 2H), 5.47 (s, 1H) 6.99 (s, 15H), 7.11 (d, 2H), 7.34 ppm (d, 2H); GPC: M_n: 4820, PDI: 1.6; ^{1}H NMR: $DP_n = 15$, M_n: 3088.

Synthesis of phenol-terminated rrP3OT (3): In a round-bottomed flask, the phenoxy-tetrahydropyranyl-terminated rrP3OT **2** was dissolved in THF (50 mL). The solution was heated to reflux and then six drops of 37 % HCl were added. The reaction mixture was heated overnight and then poured into methanol to precipitate the polymer, which was collected by filtration, washed with deionized water and methanol, and dried in vacuum. Polymer **3** was recovered in quantitative yield. ^{1}H NMR (400 MHz, $CDCl_3$): $\delta_H = 0.88$ (t, 45H), 1.28 (m, 120H), 1.41 (m, 30H), 1.70 (t, 30H), 2.80 (t, 30H), 6.99 (s, 15H), 7.07 (d, 2H), 7.26 ppm (d, 2H); GPC: M_n: 4760, PDI: 1.6; ^{1}H NMR: $DP_n = 15$, M_n: 3004.

Synthesis of aminoethanol-modified SWNT (4): A suspension of pristine SWNTs (50 mg) in DMF (50 mL) was sonicated for 10 min and then 2-aminoethanol (3 mL, 49.8 mmol) was added. The reaction mixture was stirred at 80 °C for 5 days, and then filtered through a Millipore membrane (PTFE, 0.22 μm). The collected material was washed with DMF, dichloromethane, and diethyl ether and dried under high vacuum to afford 35 mg of compound **4**.

Synthesis of rrP3OT-co-SWNT (5): Phenol-terminated rrP3OT **3** (22 mg), aminoethanol-modified SWNT **4** (15 mg), and triphenylphosphine (TPP) (20.06 mg, 0.076 mmol) were combined in a previously degassed round-bottomed flask. DMF (10 mL) and THF (10 mL) were added and the reaction mixture was sonicated for 15 min. Diisopropylazodicarboxylate (DIAD) (15 μL, 0.076 mmol) was then added and the flask was degassed and filled with argon several times. The reaction mixture was stirred at

80 °C for 24 h under argon atmosphere. The same amounts of TPP and DIAD were then added to the flask once more and the resulting mixture was allowed to react at 80 °C for a further 24 h under argon atmosphere. After being cooled to room temperature, the suspension was sonicated and centrifuged in order to remove any unreacted **4**. The supernatant was filtered through a Millipore membrane (PTFE, 0.22 μm), and the brownish solid collected was washed several times with DMF, chloroform (in order to remove any excess **3**), and diethyl ether, affording 32 mg of compound **5**. The solubility of this material was found to be 1 mg/3 mL in *o*-dichlorobenzene or 1 mg/10 mL in chloroform. FTIR (KBr): $\tilde{\nu}=2926$, 2853 cm^{-1}.

Synthesis of rrP3OT macroinitiator (6): In a degassed round-bottomed flask, **3** (195 mg) was dissolved in distilled dichloromethane (30 mL). The polymer solution was cooled to 0 °C. Chloropropionyl chloride (CPC) (0.22 mL) and distilled triethylamine (Et_3N) (70 μL) were then added and after 10 min the mixture was heated at 80 °C for 24 h. It was then cooled to 0 °C, whereupon the same amounts of CPC and Et_3N were added once more. After 10 min, the mixture was heated at 80 °C for a further 24 h. This procedure was repeated once more, and the final mixture was left to react at 80 °C for 48 h. Finally, an excess of MeOH was added to the flask and the resulting mixture was stirred for 1 h. The mixture was filtered, and the collected initiator was repeatedly washed with MeOH before being dried to afford **6** in quantitative yield. ^1H NMR (400 MHz, $CDCl_3$): $\delta=0.88$ (t, 45H), 1.28 (m, 120H), 1.41 (m, 30H), 1.70 (t, 30H), 1.84 (dd, 3H), 2.81 (t, 30H), 4.64 (m, 1H), 6.99 (s, 15H), 7.04 (d, 2H), 7.20 ppm (d, 2H); GPC: M_n: 4870, PDI: 1.7; ^1H NMR: DPn = 15, M_n: 3091.5.

Synthesis of rrP3OT-SWNT (7): The rrP3OT macroinitiator **6** (30 mg), CuBr (6.66 μmol), and bpy (13.13 μmol) were placed in a reaction flask, which was degassed and filled with argon three times. *o*-Dichlorobenzene (8 mL) and SWNT (30 mg) were then added to the flask and the mixture was sonicated for 15 min. The mixture was then heated at 110 °C for 3 d. After being cooled to room temperature, the suspension obtained was sonicated and centrifuged in order to remove any unreacted SWNT. The supernatant was filtered through a Millipore membrane (PTFE, 0.22 μm), and the brownish solid collected was washed several times with DMF, THF (in order to remove any unreacted **6**), and diethyl ether, to afford 31 mg of compound **7**. FTIR (KBr): $\tilde{\nu}=2926$, 2853 cm^{-1}.

Acknowledgements

Financial support of this work from the European Commission through the NMP3-CT-2006–033228 program and the CNTCOMP of the Marie Curie Actions (MTKD-CT-2005–029876) is acknowledged.

[1] N. S. Sariciftci, L. Smilowitz, A. J. Heeger, F. Wudl, *Science* **1992**, *258*, 1474.

[2] a) Y. Kim, S. Cook, S. M. Tuladhar, S. A. Choulis, J. Nelson, J. R. Durrant, D. D. C. Bradley, M. Giles, I. McCulloch, C.-S. Ha, M. Ree, *Nat. Mater.* **2006**, *5*, 197; b) G. Li, V. Shrotriya, J. Huang, Y. Yao, T. Moriarty, K. Emery, Y. Yang, *Nat. Mater.* **2005**, *4*, 864; c) K. Kim, J. Liu, M. A. G. Namboothiry, D. L. Carroll, *Appl. Phys. Lett.* **2007**, *90*, 163511.

[3] a) J. Peet, J. Y. Kim, N. E. Coates, W. L. Ma, D. Moses, A. J. Heeger, G. C. Bazan, *Nat. Mater.* **2007**, *6*, 497; b) D. Mühlbacher, M. Scharber, M. Morana, Z. Zhu, D. Waller, R. Gaudiana, C. Brabec, *Adv. Mater.* **2006**, *18*, 2884; c) N. Blouin, A. Michaud, D. Gendron, S. Wakim, E. Blair, R. Neagu-Plesu, M. Belletête, G. Durocher, Y. Tao, M. Leclerc, *J. Am. Chem. Soc.* **2008**, *130*, 732; d) A. Gadisa, W. Mammo, L. M. Andersson, S. Admassie, F. Zhang, M. R. Andersson, O. Inganäs, *Adv. Funct. Mater.* **2007**, *17*, 3836; e) E. Bundgaard, F. C. Krebs, *Macromolecules* **2006**, *39*, 2823; f) M. M. Wienk, M. G. R. Turbiez, M. P. Struijk, M. Fonrodona, R. A. J. Janssen, *Appl. Phys. Lett.* **2006**, *88*, 153511; g) B. C. Thompson, Y.-G. Kim, T. D. McCarley, J. R. Reynolds, *J. Am. Chem. Soc.* **2006**, *128*, 12714.

[4] E. Kymakis, G. A. J. Amaratunga, *Appl. Phys. Lett.* **2002**, *80*, 112.

[5] a) V. Sgobba, G. M. A. Rahman, D. M. Guldi, N. Jux, S. Campidelli, M. Prato, *Adv. Mater.* **2006**, *18*, 2264; b) D. M. Guldi, G. M. A. Rahman, M. Prato, N. Jux, S. Qin, W. Ford, *Angew. Chem.* **2005**, *117*, 2051; *Angew. Chem. Int. Ed.* **2005**, *44*, 2015; c) J. Geng, T. Zeng, *J. Am. Chem. Soc.* **2006**, *128*, 16827; d) S. Bhattacharyya, E. Kymakis, G. A. J. Amaratunga, *Chem. Mater.* **2004**, *16*, 4819; e) G. M. A. Rahman, D. M. Guldi, R. Cagnoli, A. Mucci, L. Schenetti, L. Vaccari, M. Prato, *J. Am. Chem. Soc.* **2005**, *127*, 10051; f) D. M. Guldi, G. M. A. Rahman, F. Zerbetto, M. Prato, *Acc. Chem. Res.* **2005**, *38*, 871.

[6] a) D. Tasis, N. Tagmatarchis, A. Bianco, M. Prato, *Chem. Rev.* **2006**, *106*, 1105; b) Y.-P. Sun, K. Fu, Y. Lin, W. Huang, *Acc. Chem. Res.* **2002**, *35*, 1096; c) M. Holzinger, J. Abraham, P. Whelan, R. Graupner, L. Ley, F. Hennrich, M. Kappes, A. Hirsch, *J. Am. Chem. Soc.* **2003**, *125*, 8566.

[7] a) J. Chen, M. A. Hamon, H. Hu, Y. Chen, A. M. Rao, P. C. Eklund, R. C. Haddon, *Science* **1998**, *282*, 95; b) V. Georgakilas, K. Kordatos, M. Prato, D. M. Guldi, M. Holzinger, A. Hirsch, *J. Am. Chem. Soc.* **2002**, *124*, 760; c) M. Ángeles Herranz, N. Martín, S. Campidelli, M. Prato, G. Brehm, D. M. Guldi, *Angew. Chem.* **2006**, *118*, 4590; *Angew. Chem. Int. Ed.* **2006**, *45*, 4478.

[8] a) J. Chen, H. Liu, W. A. Weimer, M. D. Halls, D. H. Waldeck, G. C. Walker, *J. Am. Chem. Soc.* **2002**, *124*, 9034; b) F. J. Gomez, R. J. Chen, D. Wang, R. M. Waymouth, H. Dai, *Chem. Commun.* **2003**, 190; c) H. J. Barraza, F. Pompeo, E. A. O'Rear, D. E. Resasco, *Nano Lett.* **2002**, *2*, 797; d) M. Ángeles Herranz, C. Ehli, S. Campidelli, M. Gutiérrez, G. L. Hug, K. Ohkubo, S. Fukuzumi, M. Prato, N. Martín, D. M. Guldi, *J. Am. Chem. Soc.* **2008**, *130*, 66.

[9] a) A. Star, D. W. Steuerman, J. R. Heath, J. F. Stoddart, *Angew. Chem.* **2002**, *114*, 2618; *Angew. Chem. Int. Ed.* **2002**, *41*, 2508; b) C. Richard, F. Balavoine, P. Schuitz, T. W. Ebbesen, C. Mioskowski, *Science* **2003**, *300*, 775; c) M. Numata, M. Asai, K. Kaneko, A.-H. Bae, M. Hasegawa, K. Sakurai, S. Shinkai, *J. Am. Chem. Soc.* **2005**, *127*, 5875.

[10] a) P. Mansky, Y. Liu, E. Huang, T. P. Russell, C. Hawker, *Science* **1997**, *275*, 1458; b) B. Zhao, W. Brittain, *Prog. Polym. Sci.* **2000**, *25*, 677.

[11] a) S. Campidelli, C. Sooambar, E. L. Diz, C. Ehli, D. M. Guldi, M. Prato, *J. Am. Chem. Soc.* **2006**, *128*, 12544; b) C. Cioffi, S. Campidelli, C. Sooambar, M. Marcaccio, G. Marcolongo, M. Meneghetti, D. Paolucci, F. Paolucci, C. Ehli, G. M. A. Rahman, V. Sgobba, D. M. Guldi, M. Prato, *J. Am. Chem. Soc.* **2007**, *129*, 3938.

[12] a) M. Jeffries-EL, G. Sauve, R. D. McCullough, *Macromolecules* **2005**, *38*, 10346; b) M. Jeffries-EL, G. Sauve, R. D. McCullough, *Adv. Mater.* **2004**, *16*, 1017.

[13] N. Miyaura, A. Suzuki, *Chem. Rev.* **1995**, *95*, 2457.

[14] a) E. V. Basiuk, M. Monroy-Pelaez, I. Puente-Lee, V. A. Basiuk, *Nano Lett.* **2004**, *4*, 863; b) Y. Lin, A. M. Rao, B. Sadanadan, E. A. Kenik, Y.-P. Sun, *J. Phys. Chem. B* **2002**, *106*, 1294; c) W. Wu, N. V. Tsarevsky, J. L. Hudson, J. M. Tour, K. Matyjaszewski, T. Kowalewski, *Small* **2007**, *3*, 1803.

[15] R. Graupner, *J. Raman Spectrosc.* **2007**, *38*, 673.

[16] a) O. Mitsunobu, *Synthesis* **1981**, 1; b) R. Mengel, M. Bartke, *Angew. Chem.* **1978**, *90*, 725; *Angew. Chem. Int. Ed. Engl.* **1978**, *17*, 679; c) S. Dandapani, D. P. Curran, *Chem. Eur. J.* **2004**, *10*, 3130; d) R. Dembinski, *Eur. J. Org. Chem.* **2004**, 2763.

[17] a) P. Zhou, G.-Q. Chen, H. Hong, F.-S. Du, Z.-C. Li, F.-M. Li, *Macromolecules* **2000**, *33*, 1948; b) C. L. Chochos, J. K. Kallitsis, V. G. Gregoriou, *J. Phys. Chem. B* **2005**, *109*, 8755; c) F. Giacalone, N. Martin, *Chem. Rev.* **2006**, *106*, 5136.

[18] G. Mountrichas, S. Pispas, N. Tagmatarchis, *Chem. Eur. J.* **2007**, *13*, 7595.

[19] M. Trznade, M. Zagorska, M. Lapkowski, G. Louarn, S. Lefrante, A. Pron, *Annu. Rep. Prog. Chem. J. Chem. Soc. Faraday Trans. Zeitschrift wurde bereits 1966 stillgelegt!* **1996**, *92*, 1387.

[20] M. S. Dresselhaus, G. Dresselhaus, R. Saito, A. Jorio, *Phys. Rep.* **2005**, *409*, 47.

[21] a) M. C. Iovu, E. E. Sheina, R. R. Gil, R. D. McCullough, *Macromolecules* **2005**, *38*, 8649; b) T. A. Chen, X. Wu, R. D. Rieke, *J. Am. Chem. Soc.* **1995**, *117*, 233.
[22] a) P. Chen, X. Wu, X. Sun, J. Lin, W. Ji, K. L. Tan, *Phys. Rev. Lett.* **1999**, *83*, 2548; b) Y.-Q. Wang, P. A. Sherwood, *Chem. Mater.* **2004**, *16*, 5427.
[23] S. Suzuki, C. Bower, Y. Watanabe, O. Zhou, *Appl. Phys. Lett.* **2000**, *76*, 4007.
[24] P. Dannentun, M. Boman, S. Stafstrom, W. R. Salaneck, R. Lazzaroni, C. Fredriksson, J. L. Brédas, R. Zamboni, C. Taliani, *J. Chem. Phys.* **1993**, *99*, 664.
[25] J. Heeg, C. Kramer, M. Wolter, S. Michaelis, W. Plieth, W.-J. Fischer, *Appl. Surf. Sci.* **2001**, *180*, 36.
[26] a) C. L. Chochos, S. P. Economopoulos, V. Deimede, V. G. Gregoriou, M. T. Lloyd, G. G. Malliaras, J. K. Kallitsis, *J. Phys. Chem. C* **2007**, *111*, 10732; b) A. K. Andreopoulou, J. K. Kallitsis, *Macromolecules* **2002**, *35*, 5808.
[27] R. Miyakoshi, A. Yokoyama, T. Yokozawa, *J. Am. Chem. Soc.* **2005**, *127*, 17542.

Received: April 10, 2008
Published online: August 4, 2008

